Image De-blurring Using Shearlets

Amirhossein Firouzmanesh
Department of Computing Science
University of Alberta
Edmonton, AB, Canada
e-mail: firouzma@ualberta.ca

Pierre Boulanger
Department of Computing Science
University of Alberta
Edmonton, AB, Canada
e-mail: pierreb@ualberta.ca

***Abstract*— In this paper a deblurring algorithm is proposed that takes advantage of the properties of the shearlet transform. Shearlets have mathematically been proven to be more efficient than traditional wavelets for representing distributed discontinuities such as edges. The proposed method extends the state of art ForWaRD algorithm by incorporating shearlets. Experimental results show a significant improvement over some important deblurring algorithms found in the literature.**

Keywords-Image De-blurring, De-convolution, Shearlet Transform.

I. INTRODUCTION

One of the fundamental problems in image processing is image restoration or the process of estimating the original image from a degraded image based on some knowledge of the degradation function. Some of most important applications of image restoration include astronomy, medical imaging, and seismic imaging [9]. Deblurring is an important case of image restoration in which degradation is modelled by convolving the original image with a low-pass filter, followed by the corruption of the blurred image by an additive noise.

In this paper, we consider the discrete-time two-dimensional deblurring in which the observed image $y(n_1, n_2)$ is a result of the degradation of the unknown original image $x(n_1, n_2)$ by the convolution of a linear time-invariant (LTI) filter $h(n_1, n_2)$, followed by the corruption of the filtered image by a zero-mean additive white Gaussian noise (AWGN) $\gamma(n_1, n_2)$ with variance σ^2:

$$y(n_1, n_2) = (x \circledast h)(n_1, n_2) + \gamma(n_1, n_2) \quad (1)$$

In the discrete Fourier transform domain (DFT) Equation 1 can be written as:

$$Y(k_1, k_2) = X(k_1, k_2)H(k_1, k_2) + \Gamma(k_1, k_2). \quad (2)$$

Since $H(k_1, k_2)$ typically contains values near zero the problem is said to be ill-conditioned which means one cannot obtain a good estimate of the original image by simply dividing both sides of Equation 2 by $H(k_1, k_2)$. The most common solution is to solve the problem by regularizing $H(k_1, k_2)^{-1}$. For example if we define $T(k_1, k_2)$ such that it is nearly one when $H(k_1, k_2)$ is large, near zero when $H(k_1, k_2)$ is small, and $H(k_1, k_2)^{-1}T(k_1, k_2)$ is defined everywhere else then an estimate of the original image in the Fourier domain can be expressed by: $H(k_1, k_2)^{-1}T(k_1, k_2)Y(k_1, k_2)$.

In general there is a trade-off between getting an accurate estimate of the signal and the ability to reduce noise. Different deblurring methods tries to remove the noise from the image approximation without throwing away information (see [6] for a more in depth discussion).

It is proved in [6] that if an image is a piecewise smooth function with C^2 -continuous boundaries between the regions, then the decay rate of a wavelet domain image reconstruction is $O(M^{-1})$ while for a Fourier domain reconstruction the decay rate is $O\left(M^{-\frac{1}{2}}\right)$. This means that wavelet reconstruction function is far superior to Fourier domain from the perspective of noise removal. Discrete shearlet transform described in [2] are even more efficient with a decay rate of $O(M^{-2}(logM)^3)$. As discussed in [6], good reconstruction can be obtained by combining a representation that is "effective for regularizing the inversion of the blurrig operator" and a representation effective at removing colored noise from the "approximate inversion of the operator" [10].

In this paper, we propose a new deblurring method that takes the advantages of compact representation and fast decay rate of the shearlet transform. The rest of the paper is organized as follows. The related work is briefly reviewed in Section 2. In Section 3, we introduce the shearlet transform and its unique properties for compact representation of images. The proposed method is described in Section 4 followed by a description of the implementation details and optimal parameter selection in Section 5. In Section 6, we present the results of applying the proposed method to images distorted with different type of blurring filters and different levels of noise. We then compare this result with two state of art deblurring algorithms namely ForWaRD and Wiener filtering.

II. RELATED WORK

Hansen [5] describes several deblurring methods based on filtering Singular Value Decomposition (SVD) including Tikhonov, truncated SVD, and Wiener filtering. Donoho et

al. [1] proposed Wavelet-Vagulette (WVD) deblurring technique that increases the performance of SVD-based methods by incorporating wavelet based estimators. However this method fails to provide a reasonable output for some types of blurring filters.

In 2004, Neelamani et al. [9] proposed a hybrid Fourier-wavelet regularized deblurring algorithm (ForWaRD) that works with any type of blurring filter. This method combines regularized inversion in the Fourier domain followed by noise reduction in the wavelet domain such that the image distortion is minimized. More recently Patel et al. [10] proposed a method that estimates the image using shearlet decomposition. Their method involves Fourier regularized inversion of the shearlet domain followed by generalized cross validation (GCV) for noise removal. Good estimate are obtained by incorporating highly redundant non-subsampled implementation of the discrete shearlet transform.

Pesquet et. al. [13] proposed a deblurring method based on Stein's unbiased risk estimator (SURE). They formulate the restoration problem as a nonlinear estimation problem which can be solved using the SURE method.

The literature of iterative deblurring methods is vast. We refer the reader to [10] for a review of the iterative methods. While some of the iterative methods might produce higher quality estimates of the original signal, their execution times are typically longer than non-iterative (direct) methods (see [8] as an example). Also, the output of direct methods can be used as the initial estimate for iterative methods [9]. In this paper, we compare our results with two other direct popular deblurring methods namely the Wiener and the ForWaRD algorithms.

III. SHEARLET TRANSFORM

A. 3.1 Continuous Shearlet Transform

In two-dimensional space shearlets are defined as:

$$\psi_{a,s,t} = \left|\det M_{a,s}\right|^{-\frac{1}{2}} \psi\left(M_{a,s}^{-1}x - t\right) \quad (3)$$

where $M_{a,s} = \begin{pmatrix} a & \sqrt{a}s \\ 0 & \sqrt{a} \end{pmatrix} = B_s A_s$, $A_s = \begin{pmatrix} a & 0 \\ 0 & \sqrt{a} \end{pmatrix}$, and $B_s = \begin{pmatrix} 1 & s \\ 0 & 1 \end{pmatrix}$. The matrix A_s is an anisotropic dilation and B_s is a shearing matrix. ψ is called the generating function. The shearlet transform of a function *f* is defined by:

$$SH_\psi f(a,s,t) = \langle f, \psi_{a,s,t} \rangle \quad (4)$$

If the generating function ψ satisfies a series of conditions (described below) each function $f \in L^2(R^2)$ can be reconstructed by:

$$f = \int_{R^2} \int_{-\infty}^{\infty} \int_0^{\infty} \langle f, \psi_{a,s,t} \rangle \, \psi_{a,s,t} \frac{da}{a^3} ds dt \quad (5)$$

where ψ is defined such that in the frequency domain $\hat{\psi}(\xi_1, \xi_2) = \hat{\psi}_1(\xi_1)\hat{\psi}_2(\xi_2/\xi_1)$. $\hat{\psi}_1$ and $\hat{\psi}_2$ are smooth functions inside a support of domain $[-2,-(1/2)] \cup [(1/2),2]$ for $\hat{\psi}_1$and the support of $[-1,1]$ for $\hat{\psi}_2$ is. So for $\xi = (\xi_1, \xi_2)$,

$$\hat{\psi}_{a,s,t}(\xi_1, \xi_2) = a^{3/4} e^{-2\pi i \xi t} \hat{\psi}_1(a\xi_1)\hat{\psi}_2\left(a^{-\frac{1}{2}}\left(\frac{\xi_2}{\xi_1} - s\right)\right) \quad (6)$$

which has support in:

$\{(\xi_1, \xi_2) : \xi_1 \in [-(2/a), -(1/2a)] \cup [1/2a, 2/a]$, $|(\xi_2/\xi_1) - s| \leq \sqrt{a}\}$.

In other words the support of each $\psi_{a,s,t}$ in the frequency domain is a pair of trapezoids which are symmetric with respect to the origin and oriented along a line with slope *s*.

In [4] it is shown that the shearlet coefficients of large magnitude come from edges. Also, noise spikes and edges can be distinguished by the decay rate across scales.

B. Discrete Shearlet transform

If we choose a to be 2^{-j} and $s = -l$ where $j, l \epsilon Z$ and replace $t \epsilon R^2$ with a point $k \in Z^2$, one can obtain the discrete form of the shearlets defined by:

$$\psi_{j,l,k} = |\det A_0|^{\frac{j}{2}} \psi\left(B_0^l A_0^j x - k\right) \quad (7)$$

where the matrices $A_0 = \begin{pmatrix} 4 & 0 \\ 0 & 2 \end{pmatrix}$ and $B_0 = \begin{pmatrix} 1 & 1 \\ 0 & 1 \end{pmatrix}$.

If ψ is chosen appropriately, the discrete shearlets form a tight Parseval frame bounded to 1, *i.e.*

$$\sum_{j \epsilon Z, l \epsilon Z, k \epsilon Z^2} \left|\langle f, \psi_{j,l,k} \rangle\right|^2 = \|f\|^2 \quad (8).$$

It has been shown in [4] that for images consisting of piecewise smooth regions with C^2 continuity between regions the mean square error of the reconstructed image using *M* largest shearlet coefficients is of the order $O(M^{-2}(logM)^3)$.

C. Compact Support Shearlet Frames

Lim [7] proposed an implementation of discrete shearlet transform based on a multi-resolution analysis (MRA). Their implementation has the following properties: (1) the wavelets are localized in both space and frequency domain as opposed to other implementations of shearlets which have unbounded support in the frequency domain; (2) the discrete implementation preserves useful mathematical properties similar to their continuous counterpart; (3) they produce numerically stable reconstructions.

They define the extended discrete shearlet transform (DST) as a set of subbands $(\hat{S}_{-2^M}, \ldots, \hat{S}_{2^M}, \hat{\tilde{S}}_{-2^M}, \ldots, \hat{\tilde{S}}_{2^M})$ for a user defined M $(M > 0)$, where each subband is obtained by applying an anisotropic discrete wavelet (ADWT) transform in the horizontal direction (for $\hat{S}_k$) or the vertical direction (for $\hat{\tilde{S}}_k$) on discrete shear transform of the input image.

IV. PROPOSED METHOD

In order to get an estimate of the original signal one can multiply both sides of Equation 2 by the pseudo-inverse of *H*. A suitable choice for the pseudo-inverse is called Fourier-based Regularized Deconvolution (FoRD) which can be expressed as:

$$P(k_1,k_2) = \frac{1}{H(k_1,k_2)} \frac{|H(k_1,k_2)|^2}{|H(k_1,k_2)|^2 + \Lambda(k_1,k_2)} = \frac{\overline{H}(k_1,k_2)}{|H(k_1,k_2)|^2 + \Lambda(k_1,k_2)} \quad (9)$$

where $\Lambda(k_1,k_2)$ is called the regularization term. Different FoRD techniques differ in the choice of the

regularization term. In LTI Wiener deblurring algorithm $\Lambda(k_1,k_2)$ is set to $\alpha\frac{N\sigma^2}{X(k_1,k_2)}$ where σ^2 is the variance of the noise and α is the regularization parameter. Tikhonov-regularized deconvolution uses a constant τ as the regularization term. Multiplying Equation 2 by Equation 3 one gets:

$$P(k_1,k_2)Y(k_1,k_2) = P(k_1,k_2)X(k_1,k_2)H(k_1,k_2) + P(k_1,k_2)\Gamma(k_1,k_2). \quad (10)$$

The right side of Equation 10 consists of two terms. The first term is an estimate of the original image and the second term is the residual noise. In this paper, we extend the Fourier-Wavelet Regularized Dconvolution (ForWaRD) approach [9] by incorporating shearlets instead of wavelets. The FoRWaRD approach combines the strengths of the Fourier domain representation for regularized deblurring and wavelet approximation for noise removal.

In the shearlet domain, noise removal can be done by either thresholding or applying Wiener filter to each coefficient. A relatively good approximation can be obtained by setting the threshold to $\rho\sigma_{j,l}$ where $\sigma_{k,l}^2$ is the noise variance of the shearlet subband and ρ is a constant. Wiener filtering in the shearlet domain can be defined as

$$\tilde{S}_{j,l,k} = \tilde{S}_{j,l,k}\frac{\left|S_{j,l,k}\right|^2}{\left|S_{j,l,k}\right|^2+\sigma_{j,l}^2} \quad (11)$$

where $S_{j,l,k}$ and $\tilde{S}_{j,l,k}$ are the coefficients of the original and the estimate image respectively. In practice, one does not know the shearlet coefficients of the original signal. However the original image can be estimated by applying a hard threshold to the noisy estimate. The best results can be obtained by incorporating both thresholding and wiener filtering at the same time.

The proposed method can be described as following (see Fig. 1):

1) Find the noisy estimate of the original signal by applying FoRD to the observed image;
2) Find the estimate of the original signal by applying thresholding to the shearlet coefficients of the noisy estimate;
3) Find an improved estimate by applying Wiener filtering to the shearlet coefficients of the noisy image from step 1 using image resulting from step 2 as an estimate for the original signal.

Note that in step 2 and 3 inverse shearlet transform is applied to the filtered coefficients to obtain the estimate of the original image. The basis functions used in steps 2 and 3 must be sufficiently different [3].

In step 1, a relatively small regularization term is incorporated so that the values of $P(k_1,k_2)$ would be zero only when $H(k_1,k_2)$ is zero but close to $\frac{1}{H(k_1,k_2)}$ otherwise. This can be done by choosing a small α in Wiener deblurring or a small constant in Tikhonov-regularized deblurring. The regularization term also balances the amount of shrinkage in the Fourier and shearlet domains. The choice of the regularization term is discussed in the next section.

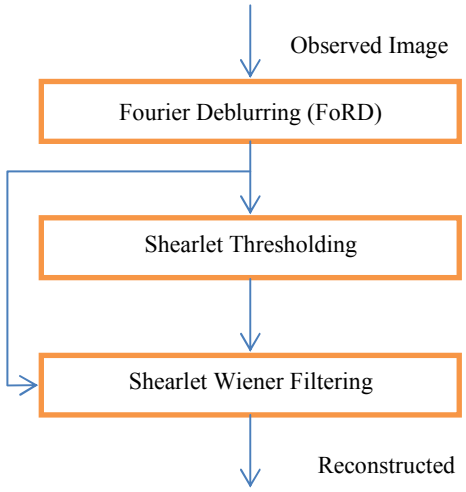

Figure 1. Block diagram of the proposed method.

The noise variance in each subband $\sigma_{j,l}^2$ can be obtained by:

$$\sigma_{j,l}^2 = \mathbb{E}\left(\left|\langle P(k)\Gamma(k),\psi_{j,l,k}\rangle\right|^2\right) \quad (12)$$

where $\mathbb{E}$ denotes the expected value, $k=(k_1,k_2)$, and $\psi_{j,l,k}$ is the basis function of the subband.

V. IMPLEMENTATION

After In this section, we discuss the selection of several parameters including regularization term, specification of the shearlet transform, and the constant ρ for thresholding.

For the shearlet domain representation, we used Shearlab [7] which implements compactly supported shearlet frames discussed in Section III.C. The input parameters are the number of scales, the size of shearlets at each scale, and the number of directions.

In the following experiments, we blurred the original image by a applying a 9x9 uniform filter and adding AWGN. In order to measure the image noise level, we used a Blurred Signal to Noise Ratio (BSNR) function which is defined as:

$$BSNR = 10\log_{10}\left(\frac{\|(x\circledast h)-\mu(x\circledast h)\|_2^2}{mn\sigma^2}\right) \quad (13)$$

where μ denotes the mean value, m and n are the image size in both directions, and σ^2 is the noise variance. For the rest of the paper, we assume that the input image is square of size n by n.

For deblurring in the Fourier domain, we use Tikhonov-regularized inversion method with constant τ set to:

$$\frac{\alpha n^2\sigma^2\|h\|_1^2}{\|y-\mu(y)\|_2^2-n(n-1)\sigma^2} \quad (14)$$

where $\|h\|_1$ is the L1-norm (sum of the largest column) of blurring filter h, and α is a parameter.

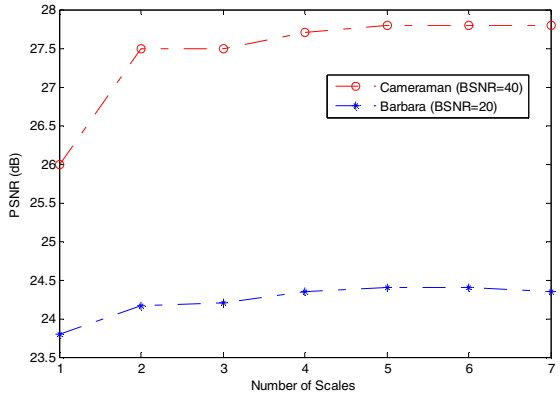

Figure 2. Number of shearlet scales vs. reconstruction quality (PSNR).

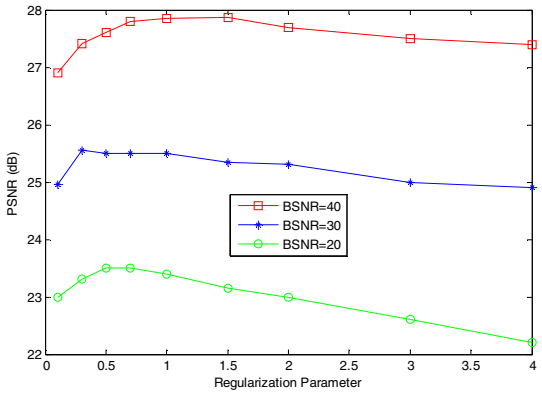

Figure 3. The effect of the regularization parameter α on the reconstruction quality.

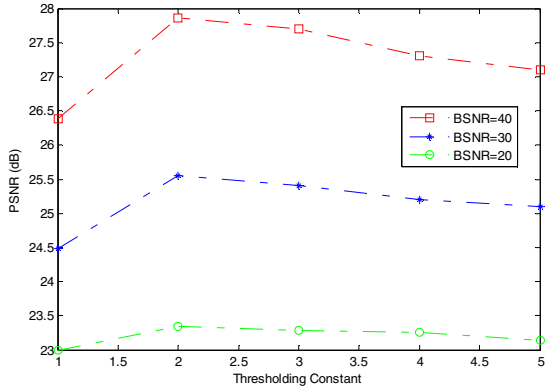

Figure 4. The effect of the thresholding parameter ρ on the reconstructed quality.

The default settings of the parameters are as follows: $\alpha = 1, \rho = 2,$ number of scales=5, the size of shearlets are $[\frac{n}{8}\times\frac{n}{2},\frac{n}{8}\times\frac{n}{4},\frac{n}{16}\times\frac{n}{8},\frac{n}{16}\times\frac{n}{8},\frac{n}{16}\times\frac{n}{8}]$ for the horizontal cone and $[\frac{n}{2}\times\frac{n}{8},\frac{n}{4}\times\frac{n}{8},\frac{n}{16}\times\frac{n}{16},\frac{n}{16}\times\frac{n}{16},\frac{n}{32}\times\frac{n}{16}]$ for the vertical cone. The number of directions is 10 for all the scales. The ADWT basis functions for steps 2 and 3 are Symmlet and Coiflet respectively.

TABLE I PSNR OF THE ESTIMATE (DB) USING DIFFERENT NUMBER OF DIRECTIONS (NDIR) FOR SHEARLET TRANSFORM

Observed Image	N-Dir=6	N-Dir=10	N-Dir=18
Cameraman (BSNR=40)	27.8	27.9	27.9
Boat (BSNR=30)	28.7	28.8	28.8
Barbara (BSNR=20)	24.3	24.4	24.4

Fig. 2 demonstrates the relationship between the number of scales for the shearlet transform and the quality of the estimate. In this experiment, we blurred the image with a 9x9 uniform filter followed by adding AWGN such that the BSNR would be between 40 and 20. One can see that increasing the number of scales from one to two has the most significant effect on the quality of the reconstructed image.

However, using more than five scales does not seem to have a considerable effect on the reconstruction quality.

The possible values for number of directions in the shearlet transform are $2^{k+2}+2$ $(k \geq 0)$. Table I presents the PSNR of the reconstructed image using 6, 10 and 18 directions. One can see that increasing the number of directions from 10 to 18 does not have any significant effect on the quality of the reconstructed image.

Table II presents the effect of using different basis functions for ADWT. The first column represents the basis function used in steps 2 and 3 respectively. The third and fourth columns are the PSNR of the reconstructed image when the input is a *Cameraman* image with BSNR=40 and *Lena* image with BSNR=20. One can see that using Coiflet for step 3 results in the best reconstruction quality.

The amount of shrinkage in Fourier and shearlet domains is balanced by setting α in Equation 14. In order to find the best value for α such that for different levels of noise the output quality is near optimal, one can apply the proposed method (with different values for α) on *Cameraman* image filtered by a 9 x 9 uniform filter. The noise variance was selected such that the BSNR would be 20, 30, and 40 dB respectively (Fig. 3). One can see that for different noise levels, choosing α between 0.5 and 1.0 result in the highest quality estimate.

In order to find the best value for the threshold constant (ρ) in step 2, we used the input setting of the previous experiment and applied our method using different values of ρ. As one can see in Fig. 4, setting ρ to a value between 2 and 3 results in the best estimate. For lower levels of noise (higher BSNRs) 2 is the best choice. As the noise level increases the difference between the qualities of the output images for $\rho = 2$ and $\rho = 3$ are less noticeable..

VI. RESULTS

In this section, we demonstrate the results of applying the proposed deblurring method to images corrupted by different types of blurring filters and different levels of noise. We also compare the performance of the proposed method with LTI Wiener deconvolution and ForWaRD algorithms. The results of the experiments are summarized in Table III.

TABLE II EFFECT OF ADWT BASIS FUNCTION ON THE RECONSTRUCTION QUALITY

Basis Functions		Input Image	
Basis function 1	**Basis function 2**	**Cameraman (BSNR=40)**	**Lena (BSNR=20)**
Daubechies	Coiflet	27.87	25.21
Daubechies	Symmlet	27.78	25.16
Coiflet	Daubechies	27.84	25.21
Coiflet	Symmlet	27.84	25.19
Symmlet	Daubechies	27.86	25.15
Symmlet	Coiflet	27.89	25.22

In the first experiment a 9x9 uniform filter was applied to a 512x512 *Barbara* image (Fig. 5a) and where a Gaussian noise with a BSNR of 40 (Fig. 5b) was added to the blurred image. One can see that for this level of blurring the deblurred image in the Fourier domain yield to a significant increase in noise. For the second experiments, the point spread function of the blurring filter was:

$$h(n_1, n_2) = \frac{1}{1+n_1^2+n_2^2} \text{ for } n_1, n_2 = -7..7 \quad (15)$$

The blurring filter was applied to a 512x512 boat image and the noise level added to the image was BSNR of 30 (Fig. 6).

In the third experiment we applied a 5x5 uniform blur to a 512x512 Barbara image. The noise variance was set to a BSNR of 30. In [13] for the same experiment the SNR of their proposed method is 0.26 dB greater than the ForWaRD method, while for our method this improvement is 0.85 dB.

In the fourth experiment a *Lena* image was blurred with the same filter as the second experiment and a noise level of BSNR of 30.

VII. CONCLUSION

In this paper, we proposed a deblurring algorithm that combines the strengths of Fourier domain for inverting the effect of the blurring filter and shearlet domain for removing the colored noise leaked from approximate inversion. As one can see at Table III incorporating shearlet transform in the deblurring process can lead to a significant improvement in the quality of the reconstructed image. This improvement is especially noticeable in images with significant amount of multidirectional edges.

A possible future research direction is to investigate the effect of using more recent noise removal techniques such as local bivariate shrinkage [11] in the shearlet domain. Also the proposed method can be adapted for specific requirements of applications such as remote sensing [12] and medical imaging [11].

TABLE III PSNR FOR DIFFERENT EXPERIMENTS

Experiment Setting	Input	Wiener	ForWaRD	Proposed
1	22.62	24.34	27.62	28.55
2	23.89	28.01	31.27	31.38
3	21.38	24.43	28.03	28.88
4	28.18	30.84	31.55	31.72

REFERENCES

[1] D. L. Donoho, "Nonlinear solution of linear inverse problems by wavelet-vaguelette decomposition," Applied and Computational Harmonic Analysis, vol. 2, pp. 101-126, 1995.

[2] G. Easley, D. Labate, W.-Qc Lim, "Sparse directional image representations using the discrete shearlet transform," Applied and Computational Harmonic Analysis, vol. 25, Issue 1, July 2008, pp. 25-46.

[3] S. Ghael, A. M. Sayeed, and R. G. Baraniuk, "Improved wavelet denoising via empirical Wiener filtering," Proc. SPIE, Wavelet Applications in Signal and Image Processing, vol. 3169, pp. 389–399, Oct.1997.

[4] K. Gou, D. Labate, "Optimally spare multidimensional representation using shearlets," SIAM J. Math. Anal., vol. 39, pp. 298-318, 2007.

[5] P. C Hansen, Rank-Deficient and Discrete Ill-posed Problems: Numerical Aspects of Linear Inversion, Philadelphia, PA:SIAM, 1998.

[6] J. Kalifa and S. Mallat, "Thresholding estimators for linear inverse problems," Ann. Statist., vol. 31, no. 1, Feb. 2003.

[7] W. Lim, "The discrete shearlet transform: A new directional transform and compactly supported shearlet frames," IEEE Trans. Image Processing, to appear.

[8] M. Mignotte, "Fusion of regularization terms for image restoration," J. Electronic Imaging, vol. 19, no. 3, 2010.

[9] R. Neelamani, H. Choi, R. Baraniuk, "ForWaRD: Fourier-wavelet regularized deconvolution for ill-conditioned systems," IEEE Trans. Signal Processing, vol. 52, no. 2, Feb. 2004.

[10] V. M. Patal, G. R. Easley, D. M. Healy, "Shearlet-based deconvolution," IEEE Trans. Image Processing, vol. 18, no. 12, Dec. 2009.

[11] M. Venu Gopala Rao, S. Vathsal, "Bi-ComForWaRD: Bivariate complex Fourier-wavelet regularized deconvolution for medical imaging," International Journal of Computational Intelligence and Applications, vol. 8, no. 2, pp. 85-95, 2009.

[12] W. Zhang, M. Zhao, Z. Wang, "Adaptive wavelet-based deconvolution method for remote sensing imaging," Applied Optics, vol. 48, no. 24, 2009

[13] J. Pesquet, A. Benazza-Benyahia, C. Chaux, "A SURE Approach for Digital Signal/Image Deconvolution Problems," IEEE Trans. Signal Processing, vol. 57, no. 12, 2009.

(a) (b) (c) (d)

Figure 5. (a) Original Image, (b) Blurred and noisy image (PSNR=22.62, BSNR=40), (c) LTI Wiener deconvolution (PSNR=24.34), (d) Proposed method (PSNR=28.55).

(a) (b)

(c) (d)

Figure 6. (a) Original Image, (b) Blurred and noisy image (PSNR=23.89, BSNR=30), (c) LTI Wiener deconvolution (PSNR=28.01), (d) Proposed method (PSNR=31.38).